

A survey on facial image deblurring

Bingnan Wang^{1,2}, Fanjiang Xu¹, and Quan Zheng¹ (✉)

© The Author(s)

Abstract When the facial image is blurred, it has a great impact on high-level vision tasks such as face recognition. The purpose of facial image deblurring is to recover a clear image from a blurry input image, which can improve the recognition accuracy and so on. General deblurring methods can not perform well on facial images. So some face deblurring methods are proposed to improve the performance by adding semantic or structural information as specific priors according to the characteristics of facial images. This paper surveys and summarizes recently published methods for facial image deblurring, most of which are based on deep learning. Firstly, we give a brief introduction to the modeling of image blur. Next, we summarize face deblurring methods into two categories, namely model-based methods and deep learning-based methods. Furthermore, we summarize the datasets, loss functions, and performance evaluation metrics commonly used in the neural network training process. We show the performance of classical methods on these datasets and metrics and give a brief discussion on the differences of model-based and learning-based methods. Finally, we discuss current challenges and possible future research directions.

Keywords Facial image deblurring, Model-based, Deep learning-based, Semantic or structural prior

1 Introduction

Facial image deblurring is a technique to recover clear facial images with sharp texture details from blurry facial images. Blurry images are widespread in life, which can be caused by various reasons, such as optical aberrations, camera shake, object movement, etc. The two most common types of

blur are motion blur and defocus blur. We show an example of blurry facial images caused by these two types respectively in Fig. 1.

With the development of technologies such as face recognition, processing degraded facial images has become an important research topic. In surveillance or some open occasions, the faces in the images are prone to motion blur which can greatly reduce the performance of systems such as face recognition and video surveillance. Therefore, facial image deblurring has become a significant research topic in computer vision, and more and more scholars have carried out research on facial image deblurring.

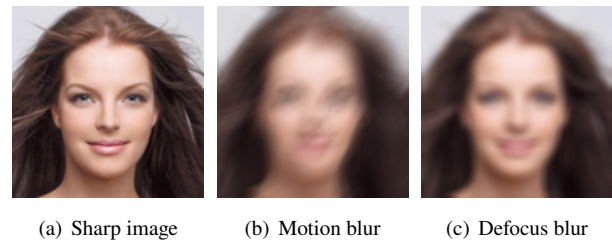


Fig. 1 Different types of blurry facial images.

1.1 Problem definition

Blur caused by many reasons, can be represented by a unified blur operator K . At the same time, considering that there may be noise in the image degradation process, we use the following model to represent the degradation process:

$$Y = D(X, K, n) \quad (1)$$

Among them, Y refers to the degraded image, X refers to the clear image, K refers to the blur operator, and n refers to the noise. In the degradation process, we consider noise to be additive. In addition, a large number of methods simplify the blur degradation process to a linear function and assume that the blur in an image is spatially invariant, so Eq. (1) can be rewritten as the following simplified model:

$$Y = k * X + n \quad (2)$$

¹ Institute of Software, Chinese Academy of Science, Beijing 100190, China. E-mail: fanjiang@iscas.ac.cn; zhengquan@iscas.ac.cn(✉).

² University of Chinese Academy of Sciences, Beijing 100049, China. E-mail: wangbingnan21@mails.ucas.ac.cn.

Manuscript received: 2022-08-17; accepted: 2023-01-19

Here, k refers to the blur kernel, and $*$ refers to the convolution operation. Image deblurring is to obtain a clear image X from a blurry image Y . According to different blurring causes, the blur kernel k can be modeled in different forms which will be described below.

Defocus blur [1]. When the object is not in the focal plane of the camera or the scene has a short depth of field, the unfocused areas can produce unclear details and textures. The point spread function of out-of-focus blur can be represented by the following model:

$$k(i, j) = \begin{cases} \frac{1}{\pi r^2} & \text{if } i^2 + j^2 \leq r^2 \\ 0 & \text{otherwise} \end{cases} \quad (3)$$

where r is the radius of the blur and (i, j) refers to the coordinates of pixels.

Motion blur. It is caused by the motion of the camera or the movement of the object. When the camera moves in a fixed direction at the moment of shooting, the blur kernel can be modeled as Eq. (4) where L is the motion length and θ is the motion angle. However, actual motion blur is more complicated than this. On the one hand, the direction and degree of movement of the camera can vary; On the other hand, in the dynamic scene, only some objects move and others are stationary. Several methods have been proposed to generate simulated blur kernels [2, 3]. However, how to ensure the diversity of simulation kernels and the authenticity of the distribution is still a problem.

$$k(i, j) = \begin{cases} \frac{1}{L} & \text{if } \sqrt{i^2 + j^2} \leq \frac{L}{2} \text{ and } \frac{i}{j} = -\tan \theta \\ 0 & \text{otherwise} \end{cases} \quad (4)$$

Gaussian blur. There are also many methods which use a simple Gaussian function in the model to represent the blurring process [4, 5]. The Gaussian kernel function can be represented by the following model where σ is the standard deviation, indicating the degree of blur:

$$k(i, j) = \frac{1}{2\pi\sigma^2} e^{-\frac{i^2+j^2}{2\sigma^2}} \quad (5)$$

1.2 Scope of this survey

Facial image deblurring is a domain-specific image deblurring problem. The corresponding solution is improved and developed on the general deblurring methods. There are some reviews [6, 7] summarizing existing general deblurring models. Among them, Li et al. [6] gave a brief summary of traditional and depth-represented image deblurring methods respectively; Zhang et al. [7] focused on the detailed introduction of deep learning-based image deblurring methods.

Different from these papers, this survey focuses on summarizing deblurring research carried out on facial images. As a special application scenario, there are less textures and edges on facial images compared to general scene images, so the proposed general deblurring methods can not produce good results on facial images. In addition, although the identity is changed, different faces are composed of fixed components which can be used as prior information to improve the performance of general methods. Based on these, a number of studies have been carried out dedicated to the deblurring of facial images, which we summarize in this article.

Before 2015, the methods used for face deblurring were mainly model-based. Some methods are proposed to improve the recognition performance, and others improve general image deblurring methods in spatial domain. Here we mainly summarize the research work carried out in the field of face deblurring after 2010. Since 2016, due to the strong fitting ability of convolutional neural network, the methods based on deep learning have been gradually proposed and achieve better performance. Therefore, we will mainly introduce the deep learning-based methods in this survey. In the deep learning model, different methods aim to introduce enough priors into the model to alleviate the problem of less facial image textures.

We show the taxonomy of involved methods in Fig. 2. Next, we will give a brief introduction of model-based methods in Section 2. Then, we summarize the learning-based methods in Section 3. Section 4 introduces the commonly used blurry-sharp facial datasets in learning-based methods. Section 5 lists the loss functions and neural network training strategies commonly used in various models. Section 6 lists the metrics used to evaluate image quality. In Section 7, we compare the performance of existing typical methods (including model-based methods and deep learning-based methods). Section 8 gives a brief discussion and macro comparison about the main differences of model-based and learning-based methods. Finally, in Section 9, we summarise the limitations of the current research and the future research directions.

2 Model-based methods

The earliest methods transformed the blurry image into frequency domain to solve the problem. Nishiyama et al. [8] addressed the blur degradation problem by learning the feature subspace of facial images in the frequency domain. The blurry images with the same point spread function (PSF) are projected into the same subspace, indicating that they have the same degree of blurring. At inference time, the kernel

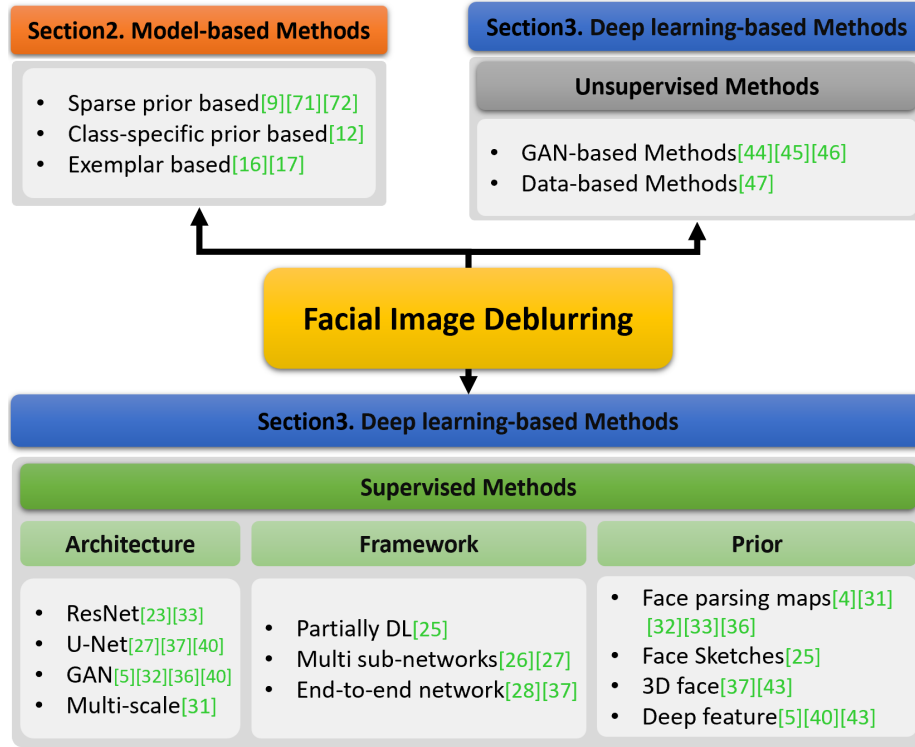


Fig. 2 The taxonomy of facial image deblurring methods concluded in our paper. “DL” represents “Deep Learning”. Details of these methods can be found in Section 2 and Section 3.

of the blurry image is determined as the PSF of the nearest subspace. However, these methods can only deal with fixed blur degradation and can not generalize to real-world blurry images with complicated and non-uniform degradation.

Most model-based methods focused on solving problems in the spatial domain. According to the degradation model established by Eq. (2), obtaining clear facial images can be expressed as the following process:

$$x, k = \arg \min_{x, k} [\|k * x - y\|_2^2 + f(x) + g(k)] \quad (6)$$

Where the first term on the right side of the equation is the fidelity term, x and y denote latent sharp images and blurry images respectively, $*$ denotes the convolution operation, and $f(x)$ and $g(k)$ are the regularization terms for the latent sharp image and the blur kernel, respectively. Since it is an ill-posed problem to simultaneously estimate the blur kernel and the sharp image from a blurry image, adding a regularization term is necessary to narrow the solution space. Eq. (6) is usually solved in an iterative way, that is estimating the blur kernel and recovering the latent image iteratively. The main idea of traditional image deblurring methods is to restore salient edges implicitly or explicitly for estimating the blur kernel k . However, in facial images, there are only few edges available for blur kernel estimation. Therefore, the existing general

deblurring methods can not achieve satisfactory results on blurry facial images.

Zhang et al. [9] adopted the sparse prior as the regularization of the latent image, and the L_2 norm prior as the regularization of the blur kernel. At the same time, a sparse representation prior was added to the face recognition process, and then clear facial images were reconstructed by jointly optimizing the process of face restoration and recognition. By combining these two tasks, a significant improvement over treating them individually was demonstrated. However, this method is only effective for facial images with good face alignment and simple motion blur. Given a specific patch of facial images, there are many similar non-local patches near it. Based on this feature, Tian et al. [10] introduced the earliest weighted non-local self-similarity (WNLSS) [11] method for denoising into the sparse representation model, and verified its effectiveness in face deblurring. Afterwards, Anwar et al. [12] proposed class-specific priors by transforming images of one specific class into Fourier space. Specifically, they learned a subspace spanned by the filter responses of sharp images in each class to a band-pass filter. In this way, the method achieves improved results when dealing with blurry images lacking high-frequency details.

Zhang et al. [13] found that in the process of iterative

optimization, some pixels of the intermediate restored image did not satisfy the model of Eq. (2), which was unfavorable for the next kernel estimation process. They proposed a pixel screening method to correct intermediate images, screening out bad pixels to facilitate more accurate kernel estimation. Tian et al. [14] updated Eq. (2) by redefining the blur kernel and latent sharp images. They represented the point spread function as a linear combination of a set of predefined orthogonal PSFs. Similarly, the estimated intrinsic (EI) sharp facial image was represented as a linear combination of a set of predefined orthogonal facial images. The coefficients of PSF and EI were jointly learned by minimizing the reconstruction error. Finally, they used a blind image quality assessment[15] method to automatically select the best images.

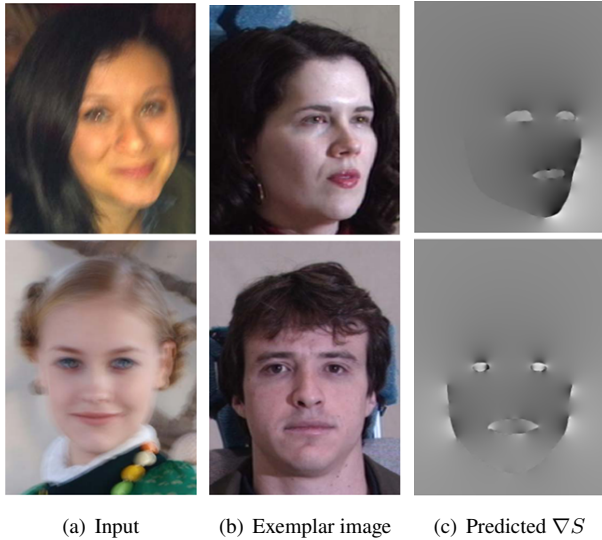


Fig. 3 Facial structures extracted from blurry input images by Pan et al. [16]. (a) Blurry facial image to be restored; (b) Matched example facial image; (c) Corresponding edge of facial structure.

In addition, some methods using reference images have been developed. Hacoen et al. [17] proposed a facial image deblurring method with the help of a reference image, where the reference image has the same scene as the original blurry image. The function of the reference image is twofold. On the one hand, information from reference images can facilitate the process of kernel estimation. On the other hand, it can be served as a strong local prior for non-blind deconvolution. The algorithm performs well in deblurring certain classes of images. However, the same reference image as the input observation has certain limitations in practical applications. Subsequently, Pan et al. [16] proposed a new method that did not require the sample and test images to have the same identity and background. The authors constructed an example dataset of facial images from the CMU PIE dataset and extracted

important structures for each image, including facial contours, eyes, and mouths. At test time, the test image was compared with the structure of the sample and the best match was found. Fig. 3 shows an example of the matched facial structure given in the paper. This structure is used to recover image edges and guide the blur kernel estimation process. After obtaining the face edge, also according to Eq. (2), the blur kernel is estimated alternately and the latent image is restored. The face structure information in this exemplar library can help extract face edges and eliminate the phenomenon of ringing and artifacts in traditional edge selection methods. However, matching each image to an example dataset is computationally intensive. Processing a single image takes hours. Also, this type of approach tends to be inaccurate for face poses and angles that are not present in the dataset.

3 Methods based on deep learning

According to [7], we can conclude that there are some commonly used basic blocks in neural networks for image deblurring, such as convolution block, ResBlock, Inception Block [18] and DenseBlock. Also, there are some commonly used network architectures such as U-Net [19], multi-scale network [20], generative adversarial network (GAN) [21], cascade network [22], etc. U-Net consists of encoder, decoder, and skip connections which can perform image transformation in an end-to-end manner. The multi-scale network feeds the original size image and the downsampled low-resolution image into the network. It first performs image restoration on small scales, and then restores images up to the original size. It performs image deblurring in a coarse-to-fine way, but greatly increases the computational load of the model. Similarly, cascaded networks can generate higher quality images due to the concatenation of networks. GAN can generate diverse and realistic facial images, but the disadvantage is that sometimes the generated sharp facial image is not the same identity as the corresponding blurry one.

To reduce the ill-posedness of the problem, Jin et al. [23] improved the basic block. They advocated to expand the range of receptive fields in Resnet [24]. They employed a resampling convolution operation that ensured a wide receptive field (RF) from the first layer while being computationally efficient. The advantages of using a large receptive field can be analyzed in two ways: first, the last few layers of the network can take advantage of higher abstract levels to better understand the image content and ultimately produce better deblurred outputs; second, a larger RF contains more structural information. And more erroneous latent image-kernel pairs can be excluded compared to using a small RF with less

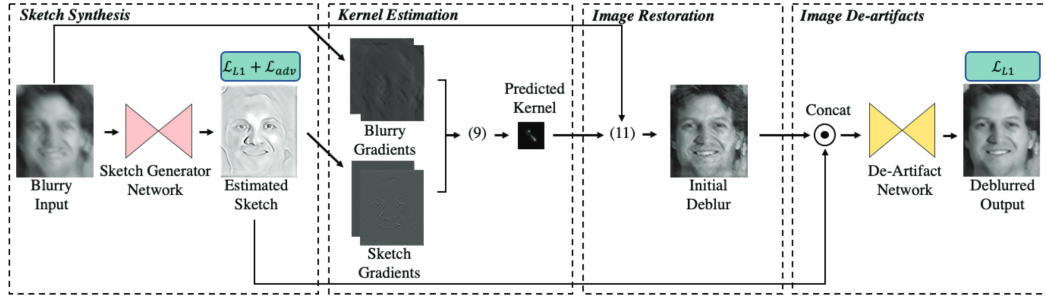


Fig. 4 An example of the first class of methods [25]. The blurry input first goes through a neural network to generate an estimated sketch. The traditional optimization process of kernel estimation and deconvolution is then performed based on the gradients of the sketch and blurry input; finally a clear output is obtained through the De-artifacts network.

structure, thereby reducing the ill-posedness of the system. To avoid artifacts, the authors concatenated a hybrid sub-network after the deblurring network, applying several convolutional layers to process local images.

Many models use a combination of the above network architectures and basic blocks to achieve good restoration of blurry faces. Next, we will summarize the deep learning methods of facial image deblurring separately according to whether paired training data is required. Also, we give a summary of these methods in Table 1.

3.1 Supervised learning

Some deep learning methods have been developed for image deblurring and applied to facial images. These methods can be roughly divided into three categories. The first class of methods first utilize the neural network to estimate blur parameters, and then restore sharp images in model-based image deblurring frameworks. Chakrabarti et al. [2] utilized a CNN to compute the complex Fourier coefficients of the deconvolution filters of each image patch, followed by non-blind deconvolution. Lin et al. [25] utilized U-Net to extract face sketches for blur kernel estimation and non-blind deconvolution. Its architecture is shown in Fig. 4.

The second class of methods use multiple sub-networks to improve the performance of deblurring results. Schuler et al. [22] used a cascaded network structure to iteratively perform kernel estimation and deconvolution processes. The algorithm adopted a coarse-to-fine strategy similar to model-based deblurring methods. However, the network does not generalize well to different and diverse kernel sizes. Xu et al. [26] constructed two sub-networks for image deconvolution and artifact removal, respectively. We show its architecture in Fig. 5. Chrysos et al. [27] adopted a two-step architecture to perform facial image deblurring. The first step used a high-performance hourglass network to recover the low and medium frequencies of the image. The second step

recovered the high-frequency details of the images by training a conditional GAN, while ensuring that the output images are close to natural images.

The third class of methods utilize an end-to-end learning approach to model the entire restoration process. Nah et al. [20] proposed a multi-scale CNN to directly perform image deblurring without an intermediate kernel estimation step. We present their model architecture in Fig. 6. Chrysos et al. [28] were the first to explicitly use deep architectures for face deblurring. The authors improved the classic Resnet architecture for performing end-to-end face deblurring tasks. Among them, face alignment techniques were used to preprocess each face, and weak supervision was inserted to exploit the structures of faces. However, during testing, the preprocessing of the blurry input is prone to errors, resulting in poor subsequent deblurring. Wang et al. [29] stacked multi-scale Inception modules in a residual way to perform face deblurring. The convolution kernels of different sizes of the Inception [18] module can deal with different blurring degrees of the input image respectively, but it brings memory consumption. Qi et al. [30] employed a generative adversarial network (GAN) architecture to explore its specific effects in face deblurring. The authors adopted an improved U-Net and a feature enhancement module as the generator. Through careful design of network basic blocks, enhanced feature representation, and adversarial training, the proposed method is able to generate more realistic faces.

There are few edges and textures in the facial images. When we only input the blurry-sharp face pairs to the model, the output deblurred facial images are not clear enough, with artifacts and poor details. On the basis of the above three types of methods, many methods have explored the effectiveness of prior information in face such as semantics for the task of deblurring. Although different faces are very multifarious, they are composed of fixed components. In order to make full use of face features, many methods focus on extracting

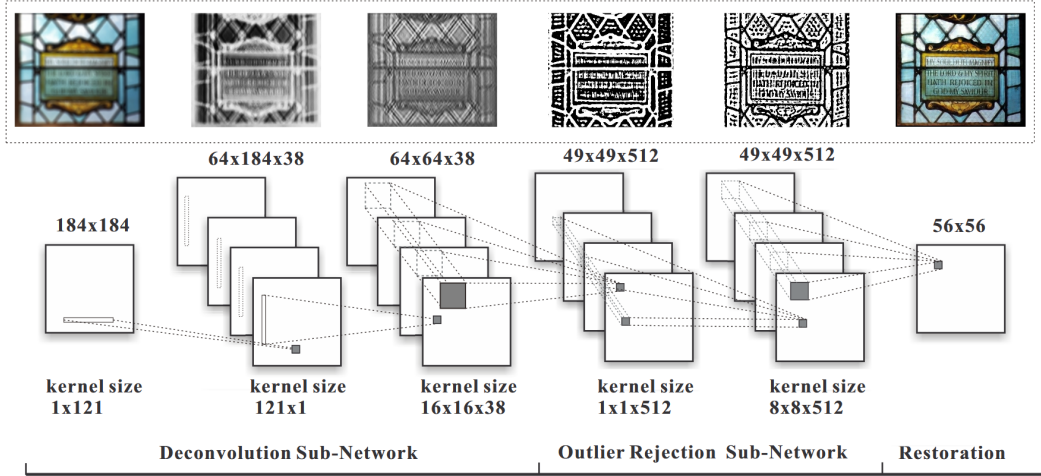


Fig. 5 An example of the second class of methods [26]. This model performs deconvolution and de-artifacting sequentially through two network modules.

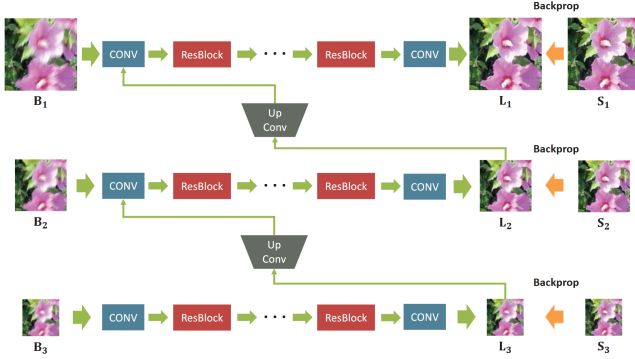


Fig. 6 An example of the third class of methods [20] which is the end-to-end deblurring neural network. This method first recovers the low-resolution blurry image B_3 , and then upsamples the result into the deblurring framework of higher-scale B_2 . Finally, the original scale image B_1 is restored.

specific information from facial images as a prior to guide network training. The priors proposed by recent studies are: facial geometry priors (such as face landmarks [28], face parsing maps [4, 31–34], 3D facial model [35, 36]) and deep feature priors [5, 36, 37].

Shen et al. [31] first attempted to incorporate the semantic parsing information of facial images into the network as a prior. We show their model architecture in Fig. 7, which is a typical model with a face semantic map as a prior. The authors adopted the deblurring network proposed by Nah et al. [20]. The authors obtained the semantic map of the blurry facial images through the semantic segmentation network, and concatenated the semantic map and the blurry image in the channel dimension as the input of the deblurring network. In order to enhance local performance, such as eyes, eyebrows, mouths, etc., the authors also proposed a local structure loss to constrain the local output of the network. However,

when there is severe motion blur in the input image, the semantic maps extracted from the blurry image are likely to be wrong. Based on this, the authors improved their work in 2020 [33]. In order to extract a correct face parsing map, the authors added a coarse deblurring network before the face parsing network to reduce the blur in the input image. Then, the face parsing network extracted semantic maps from the coarse deblurred images. Finally, the fine deblurring network recovered sharp facial images from the given blurry input images, coarse deblurred images and corresponding semantic maps. Another improvement is that in the local structure loss of face components, different weights are set for each face component separately, instead of using fixed weights for all components. This adaptive local structure loss can adjust weights and recover fine details based on the size of each facial component.

In the same year as [31], Song et al. [4] exploited semantic information to jointly perform face super-resolution and face deblurring. The model mainly consists of two modules. The first module is a deep CNN called the Facial Structure Generation Network. The network takes the degraded image and semantic masks as input and predicts a base image containing the basic structure of the face. To enhance the facial details in the base image, the authors developed a detail enhancement algorithm based on high-resolution example images. In the first step, the patch correspondence between the base image and the high-resolution (HR) example image was established, and then the base image was regressed using the patches from the HR example image and an intermediate result was obtained. In the second step, the details in the intermediate result were passed to the base image through edge-preserving filter to obtain the final result. The establishment of the detail

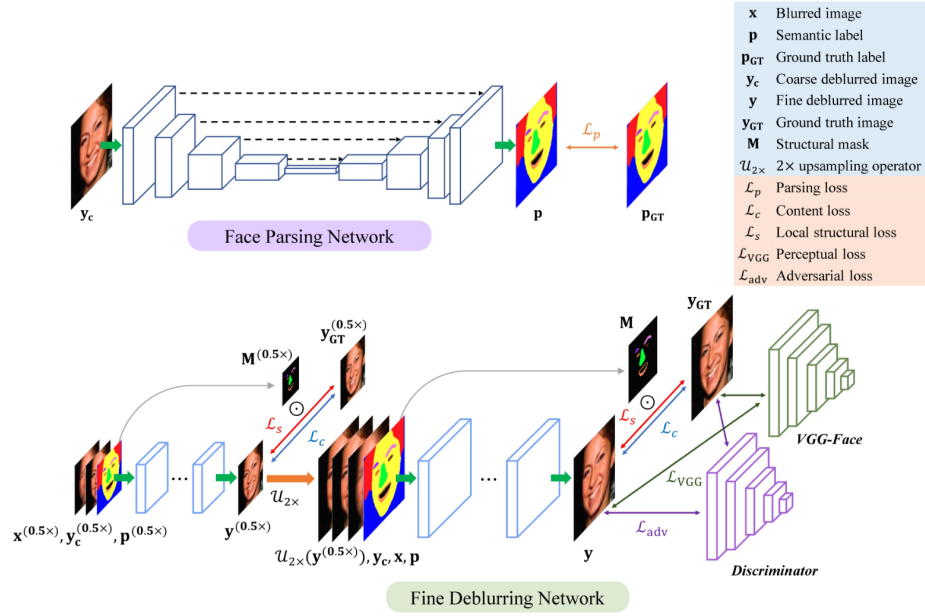


Fig. 7 Use a face semantic map as a prior for deblurring neural network [33]. This method first obtains semantic labels of blurry facial images through a face parsing network. Then the semantic map is concatenated with the blurry image in the channel dimension as the input of the deblurring network.

enhancement module ensures that even if the semantic mask extraction of the input blurry image is inaccurate, the real face with detailed edges can be recovered.

However, some facial components such as eyes, eyebrows, and mouth can not be reconstructed well due to the small face area. Yasarla et al. [32] noticed a class imbalance in the semantic map of faces. They proposed a confidence measure based multi-stream semantic network. In the first stage of the network, different streams were used to complete the semantic map feature extraction of each class. The extracted features were concatenated together and fed into the second stage and used as input together with semantic map fusion. In the second stage of the network, class-specific residual feature maps were learned by using the Nested Residual Learning (NRL) strategy. Further, the residual feature maps added to the overall blurry image were estimated. The authors introduced a confidence parameter for each class to measure the importance of each class. This parameter was predicted using a separate confidence network and was added to the loss function to reweight the contribution of each class's loss to the total loss. In this way, the trained network can offset the imbalance problem in the estimation of different classes, and then better recover the details of small areas such as nose and eyes.

When using semantic segmentation maps of faces, the accuracy of segmentation can greatly affect the performance of restoration. Moreover, it is very difficult to obtain accurate

semantic segmentation maps from blurry input images. Zhang et al. [38] employed focal loss [39] to fine-tune the face parsing network to acquire more accurate facial structure from a blurry image. They also proposed a separate normalization and adaptive denormalization block and a texture extractor to enhance the texture and facial details of the deblurred image. Lee et al. [34] proposed a method to learn facial component restoration without performing segmentation. The proposed multi-semantic progressive learning (MSPL) framework was based on the GAN structure as a whole. It introduced semantic coarse-to-fine progressive learning into the face deblurring task for the first time. In general image deblurring, progressive learning is mainly based on multi-scale network frameworks. In this model, the generator gradually generates the face components in the order of skin, hair, interior (eyes, nose, and mouth), and finally the entire face. The model's multi-semantic discriminator processed multiple outputs of the generator, which allowed to recover more realistic facial components at all intermediate layers.

In addition to face parsing maps, Lin et al. [25] used face sketches as priors to guide the blur kernel estimation process. Sketches of human faces can model global relationships, which can be used as prior information to achieve better results than extracting local sharp edges. The authors used a CNN to generate face sketches and used the learned sketches to guide the motion blur estimation module. At the same time, the generated sketches were also fed into the de-artifact

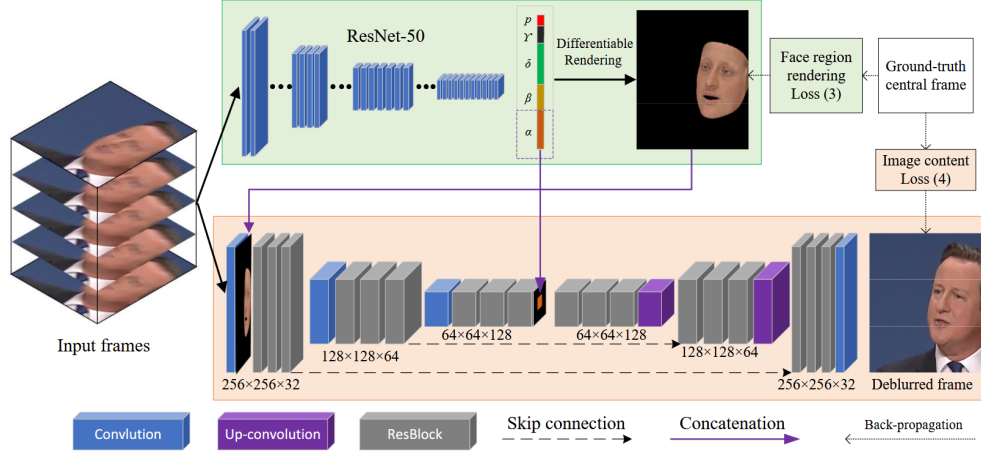


Fig. 8 Deblurring neural network using 3D human face as prior [35]. The top green block is to reconstruct a 3D face by regressing 3DMM [41] coefficients and render a sharp facial image. The bottom orange block focuses on face deblurring guided by the extracted identity vector and the rendered sharp face structure from the 3D face reconstruction branch.

subnetwork to encourage image reconstructions that preserve details and edges.

Ren et al. [35] used 3D face priors [40] as guidance information to achieve facial video deblurring. We show their network model in Fig. 8. Textured 3D faces were first generated for the center frame of the video using a 3D face reconstruction network that provides image-level (such as intensity with sharp edges) and perceptual-level (such as identity) information. The face deblurring network then applied the rendered, pose-aligned facial image as a guide to recover sharp faces. Furthermore, to encourage the generation of identity-related face details during the deblurring process, the identity vectors extracted by the 3D reconstruction network were further embedded into the deblurring network branch. Benefiting from the clear face structure estimated by 3D face rendering, the model can achieve good output results without using multi-scale structure and without using tricks such as perceptual loss.

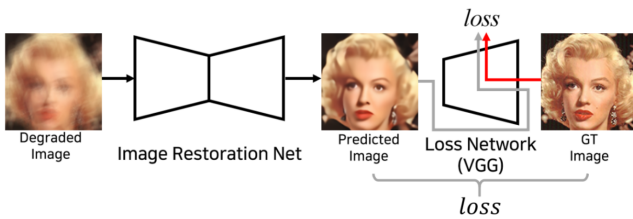


Fig. 9 Deblurring neural network using deep features as network loss [37].

In 2017, Xu et al. [42] proposed to introduce perceptual loss into the face deblurring network to guide the training of the network. The perceptual loss calculated the error between the deep features of two images. Its framework is shown in

Fig. 9. Unlike Xu, Jung et al. [37] tried to guide the deblurring process by using the deep features of the image as a separate stream in the network. Its network architecture is shown in Fig. 10. Both face geometry and texture information were included in the deep feature. In addition, a channel attention feature discriminator was also proposed to assign different importance levels to different channels of the deep feature, enabling the generator to focus on more important channels.

In 2021, Wang et al. [5] leveraged diverse generative facial priors for blind face restoration. This method also used deep features of images as prior information, the difference was that it used StyleGAN2 [43] to extract deep features. The input image was mapped to the closest latent code through an MLP. The latent code was input into the StyleGAN2 network, and its intermediate features were extracted as generative prior information, which were modulated to guide the network to obtain more realistic results. Zhu et al. [36] proposed an adaptive feature fusion block to synthesize shape feature priors and deep feature priors of images. The shape prior of the image was acquired by a 3D face reconstruction module, and the acquisition of the deep feature prior was similar to [5], which was acquired by StyleGAN2. However, these two methods focus on comprehensive degradation on facial images including blur, noise and JPEG compression. They are not designed specifically for deblurring.

In conclusion, end-to-end deblurring networks based on deep learning outperform traditional methods that require iterative optimization in speed. Properly introducing semantic information into the network will improve the deblurring accuracy of the network. The common disadvantage of these methods is that they are only suitable for processing uniform motion blur and aligned facial images. These methods may

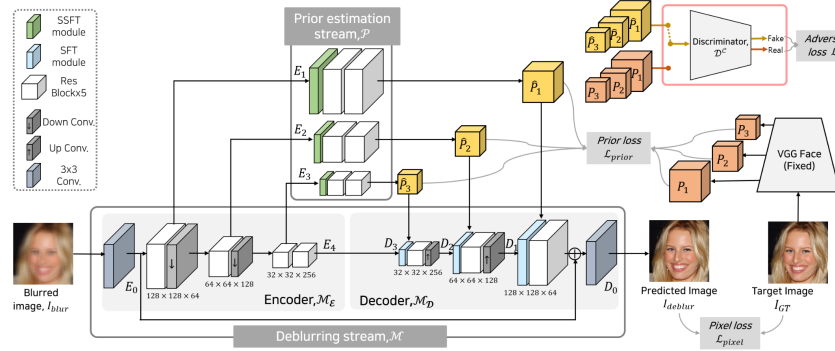


Fig. 10 Deblurring neural network using deep features of images as network prior [37]. Deep feature is extracted by prior estimation steam.

fail for non-uniform blur or face profile images.

3.2 Unsupervised Learning

On the one hand, the performance of deep neural networks strongly depends on a large number of paired training datasets, however, it is difficult to construct such paired training datasets. On the other hand, most of the current methods operate on synthetic training datasets. The learned network does not generalize well to real-world blurry images due to the large differences in data distribution between different domains. To overcome these difficulties and limitations, some researchers focus on unsupervised methods for facial image deblurring.

In 2018, Madam et al. [44] proposed a GAN-based method for unsupervised image deblurring. They added a reblur loss and a multi-scale gradient loss to the model. Although they achieved good performance on synthetic datasets, their results on some real blurry images were not satisfactory. In 2019, Lu et al. [45] proposed an unsupervised facial image deblurring method based on disentangled representation. The model separated content features and blur features from blur images, and normalized the distribution range of the extracted blur attributes by enforcing KL divergence loss, thereby realizing the decoupling of the two features. Similar to CycleGAN [46], an adversarial loss and a cycle-consistency loss were used as regularizers to help the generator network generate more realistic images while preserving the content of the original images. A perceptual loss was also added to remove artifacts in blurry images. We show its model architecture in Fig. 11.

In the same year, Xia et al. [47] proposed a data-based unsupervised framework for training image estimation networks. The framework can be applied to a general class of observation models, where measurements are linear functions of real images, accompanied by additive noise. The authors provided solutions for blind restoration and non-blind restoration, which can be used in face

deblurring. In blind image restoration, a parameter estimation network and an image estimator were trained separately, and the network was guided to learn image deblurring from unlabeled data by defining a "swap-measurement" loss and a "self-measurement" loss. The training of this framework does not require paired training data, but requires two blurry images with different blur types for the same scene.

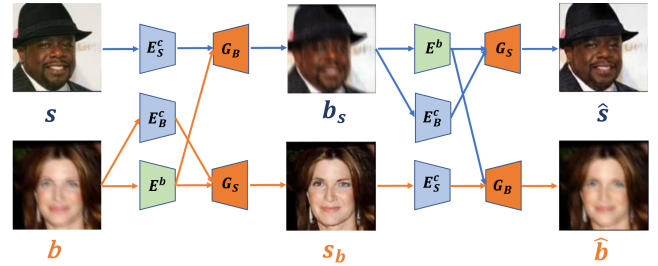


Fig. 11 Unpaired methods for facial image deblurring [45]. It adopts CycleGAN as a whole, including the blurring branch (top row) and deblurring branch (bottom row). E_B^c and E_S^c are content encoders for blurry and sharp images; E^b is the blur encoder; G_B and G_S are blurry and sharp image generators.

Unsupervised learning methods lack corresponding ground-truth images as supervision information, so the generated images are of low quality. However, it allows training on easily generated unpaired data as well as on wild images that represent real blur, so it is of great significance to develop unsupervised learning methods.

4 Datasets used for facial image deblurring

Depending on how the datasets are constructed, they can be divided into real shot datasets and synthetic datasets. For real shot datasets, the blurry images are usually obtained by averaging video frames or move the camera through a specific trajectory. For facial image deblurring, most methods are trained on synthetic blurry-sharp image pairs.

Table 1 Overview of single facial image deblurring methods.

Method	Category	Architecture	Loss	Type of Prior
Hacohen et al. [17]	Model-based	Iterative optimization	None	Reference image
Pan et al. [16]	Model-based	Iterative optimization	None	Reference image
Anwar et al. [12]	Model-based	Iterative optimization	None	Class-specific prior
Madam et al. [44]	Unsupervised	GAN, CNN	Adversarial loss; Reblurring loss; Gradient loss;	None
Lu et al. [45]	Unsupervised	GAN	Adversarial Loss; Cycle-Consistency Loss; Perceptual Loss; KL divergence loss	None
Xia et al. [47]	Unsupervised	Arbitrary	Swap-measurement loss; Self-measurement loss	None
Chrysos et al. [28]	Supervised	ResNet	Huber Loss [48]	Facial landmarks
Song et al. [4]	Supervised	CNN	L2 content loss	Facial masks
Shen et al. [31]	Supervised	GAN, Multi-scale	L1 content loss; Local structural loss; Perceptual loss; Adversarial loss	Face semantic labels
Jin et al. [23]	Supervised	ResNet	Content loss	Large receptive field
Ren et al. [35]	Supervised	ResNet, U-Net	L2 content loss; Rendering loss	Rendered 3D face
Chrysos et al. [27]	Supervised	GAN, U-Net	L1 content loss; Projection loss; Adversarial loss	None
Lin et al. [25]	Supervised	GAN	L1 content loss; Adversarial loss	Face sketches
UMSN [32]	Supervised	ResNet	Local structural loss; Perceptual loss	Face semantic labels
Shen et al. [33]	Supervised	GAN, U-Net, Multi-scale	Cross-entropy loss; L1 content loss; Local structural loss; Perceptual loss; Adversarial loss	Face semantic labels
MSPL [34]	Supervised	GAN	Local structural loss; Perceptual loss; Adversarial loss	Face semantic labels
GFP-GAN [5]	Supervised	U-Net, GAN	L1 content loss; Perceptual loss; Adversarial loss; Local structural loss; Identity preserving Loss	Generative prior in StyleGAN
Qi et al. [30]	Supervised	U-Net, GAN	L2 content loss; Perceptual loss; Adversarial loss	None
DFPGnet [37]	Supervised	U-Net, GAN	L1 content loss; Adversarial loss; Prior loss	Deep feature prior in VGGFace
SGPN [36]	Supervised	GAN	L1 content loss; Adversarial loss	Generative prior and rendered 3D face prior

4.1 Real shot datasets

2MF² dataset [28]: This dataset is created by processing and extracting faces from videos containing facial images. It consists of 1,150 videos containing 2.1 million frames of acceptable facial images, and landmark localization is

implemented for each image. The authors later updated the dataset [27], expanding the number of videos and the number of face identities in the images. The augmented dataset contains people of different ages and ethnicities and includes 19 million frames from 11,590 videos of 850

different identities, each of which appears in multiple videos. Meanwhile, the authors generated motion-blurred images by averaging multiple frames of the same face.

Lai et al. dataset [49]: Lai et al. collected real-world blurry images obtained in the wild. These images were taken by different users with different cameras and with different settings. There are a total of 100 real blurry images, including natural images, facial images and text images, all of which have no corresponding ground-truth. Various face deblurring models and methods are tested and compared on this dataset for their performance on real blurry images.

4.2 Synthetic datasets

Shen et al. dataset [31]: Shen et al. collected 2000, 2164 and 2300 clear facial images as ground truth from Helen dataset [50], CMU PIE dataset [51], CelebA dataset [52], respectively. Then 20,000 motion blur kernels are generated according to the method in [3], with sizes ranging from 13×13 to 27×27 . The corresponding blurry images are synthesized by convolving clear images with these blur kernels and adding Gaussian noise. In total, they generated 130 million blurry-sharp image training pairs. The authors also constructed a test set containing 16,000 images. It was generated by collecting 100 facial images from the validation set of the Helen and CelebA datasets, respectively, and convolving them with another 80 generated motion blur kernels.

MSPL dataset [34]: Lee et al. used 30,000 high-resolution facial images from the CelebA-HQ dataset [53] as clear ground truth and generated 18,000 motion blur kernels according to the method in [2]. They convolved the sharp image with the kernel and added gaussian noise. The generated images were split into two subsets: 24,183 image pairs for training and 5,817 image pairs for validation. The authors also collected a total of 240 clear images (80 in each dataset) from the CelebA dataset, CelebA-HQ dataset and FFHQ dataset [54] and convolved them with 240 synthetic motion blur kernels for model testing. Two types of test data were generated, MSPL-Center and MSPL-Random. Among them, MSPL-Random was generated by random rotation, cropping and horizontal flipping of MSPL-Center.

Jin et al. dataset [23]: Jin et al. collected and cropped 110,000 320×320 clear facial images from FaceScrub [55], and generated 10K random motion blur kernels according to the method in [2]. Finally, white Gaussian noise was added to generate their training data.

Lin et al. dataset [25]: Lin et al. collected 2184, 2000, 2000, and 2400 clear facial images from the CMU PIE, Helen,

CelebA, and PubFig dataset [56], respectively. These clear images were convolved with 20,000 motion blur kernels to generate blurry images. The blur kernels vary in size from 21×21 to 51×51 . To increase the diversity of the data, data augmentation was also applied, including random rotation, cropping, scaling, etc.

There are also many works that choose different datasets and blur kernel generation methods to simulate their own training or testing image pairs according to their specific application scenarios, which are summarized in Table 2. Some of them are not open to public, just used for training their model.

5 Training strategy

5.1 Loss Function

When training the network, the choice of loss function is critical to the final deblurring performance. In general deblurring models, content loss, perceptual loss and adversarial loss are often combined to achieve better results. For domain-specific face deblurring, local structure loss, identity preserving loss, etc. are also proposed to help improve the performance.

Content loss. Content loss, also known as reconstruction loss, is the most classic and commonly used loss function. Its goal is to measure the pixel-by-pixel difference between the output deblurred images and ground truth images. L_1 distance (mean absolute error) or L_2 distance (mean squared error) are often used to measure the difference. Its calculation formula is as follows:

$$L_{\text{content}} = \frac{1}{WH} \sum_{i=1}^W \sum_{j=1}^H f(I_D(i, j) - I_S(i, j)) \quad (7)$$

Where, the function f represents the L_1 distance or the L_2 distance, I_D and I_S represent the deblurred image and the corresponding sharp ground truth image, respectively, W and H represent the width and height of the image, respectively. As can be seen from the formula, the content loss calculates the distance of each pixel in the two images, and finally sums it up. When using content loss in the network, the pixel values of the deblurred output image will be as close to ground truth as possible.

However, this method of comparing differences pixel by pixel is relatively simple and crude, and does not consider human subjective visual perception. Adopting content loss tends to lead to over-smooth output results. Some methods [27, 44] also incorporate a first-order gradient distance between the deblurred image and the ground truth image in the content loss to remove undesired ringing artifacts at image boundaries.

Table 2 Overview of different datasets used for training or testing constructed by different authors.

Dataset	Synthetic	Real	Clear image source	Blur kernel source
$2MF^2$ [28]	✗	✓	none	none
Lai et al. [49]	✗	✓	none	none
Shen et al. [31]	✓	✗	Helen, CMU PIE, CelebA	[3]
MSPL [34]	✓	✗	CelebA-HQ	[2]
Jin et al. [23]	✓	✗	FaceScrub	[2]
Lin et al. [25]	✓	✗	CMU PIE, Helen, CelebA, PubFig	[3]
Madam [44] & Lu [45] & Qi [30]	✓	✗	CelebA	[2]
Wang et al. [5]	✓	✗	FFHQ	Gaussian blur kernel
Xia [47] & Yasarla [32]	✓	✗	Helen, CelebA	[2]
Song et al. [4]	✓	✗	Multi-PIE [57], PubFig	Gaussian blur kernel

Perceptual Loss. A visually pleasing result can not be achieved with content loss alone. Perceptual loss has been widely used in applications such as style transfer and image super-resolution to enhance the perceptual effect. It aims to compare the distance of deblurred and sharp images in high-dimensional feature space to measure their feature similarity. The perceptual loss can be written as:

$$L_{per} = \|\phi_l(I_D) - \phi_l(I_s)\|_2^2 \quad (8)$$

Where, ϕ_l represents the output of layer l of a pre-trained network. [4, 25, 32–34] used the outputs of *pool2* and *pool5* layers of the pretrained VGG-FACE network, while [5, 30, 37] used the outputs of *conv3_3* and other layers of the pretrained VGG-19 network as features. The low-level features in the pretrained network contain edge, color, brightness and other information, and the high-level features contain texture and rich semantic information. When the perceptual loss is used in the network, the details and texture of the output image can be enhanced. For example, the edge parts of the image will be sharper, which makes up for the over-smooth output results caused by the content loss.

Adversarial Loss. In order to make the output facial images as realistic as possible and close to natural images, many GAN-based methods have been developed. GAN-based networks define the problem as a min-max optimization process in order to make the output image of the generator close to the real face. The training objectives of generator G and discriminator D are opposite, and they generate real images by playing against each other. The adversarial loss is calculated as follows:

$$L_{adv} = E[\log D(I_S)] + E[\log(1 - D(G(I_B)))] \quad (9)$$

Where, I_B represents the blurry facial image. Through the game between the generator and the discriminator, the adversarial loss will make the output image of the network as close to the real face as possible. However, training with only adversarial loss may result in loss of details of the image (such as eyes, nose, mouth of faces). This is because the generator

can generate real images even if some details or colors are lost, and the discriminator classifies these images as real with a small adversarial loss.

Local Structural Loss. The content loss supervises the image as a whole, due to the small proportion of the face's eyes, nose, mouth and other areas in the entire image, only using the content loss can not restore these parts well. Many methods [5, 31–33] introduce a local structure loss of the face to enhance important facial components in perception. The common practice is to extract the face parsing map of the input image or directly perform face segmentation, and then apply different importance weights to different facial components. It is defined as follows:

$$L_s = \sum_{i=1}^N \omega_i \cdot \|M_i \odot I_D - M_i \odot I_s\| \quad (10)$$

Where, M_i is the semantic mask of the i -th component extracted from the facial image, and ω_i refers to the weight of the i -th component. The models typically apply local structure loss on components such as eyes, eyebrows, teeth, lips, and nose, but not on areas such as skin and hair. The introduction of a local structure loss can force the network to reconstruct sharper details in key component parts of the face.

Identity Preserving Loss. Similar to the perceptual loss, the identity preserving loss limits the distance between the deep features of two images. In [5], the authors adopt the face recognition network ArcFace[58] to extract the identity features of facial images. By limiting the distance between the identity feature of the deblurred image and the real sharp image, the deblurring result is not distorted, thereby improving the accuracy of subsequent face recognition and other tasks.

Other losses. In addition to the above losses, some specific loss functions exist to improve the performance of specific models. Unsupervised methods [44] define a reblurring loss to address the lack of ground truth images. Another unsupervised method [47] addresses the lack of training image pairs by defining "self-measurement" loss and "swap-measurement"

loss. A prior loss was introduced in [37] to ensure that the deep feature priors used to guide network training are accurate. In order to extract accurate 3D face priors, a rendering loss function is defined in [35] to make the 3D face reconstruction process unaffected by blurry images.

Each loss function has different effects on deblurred images. In the actual training process, it is necessary to comprehensively select a variety of loss functions according to the actual need of the network model to improve network performance.

5.2 Training Scheme

A face deblurring model may contain multiple sub-networks, and these sub-networks or the entire network are trained separately with various loss functions. At this time, the training strategy of the large network will also affect the final effect to a certain extent. A progressive training strategy was adopted in [33]. Firstly, they trained the sub-network. The training scheme is: with the remaining networks fixed, each sub-network is trained separately with a specific partial loss function as a coarse adjustment. Then all sub-networks, i.e. the entire model, are jointly trained by minimizing the overall loss.

Besides, to improve the model performance and enable it to handle random blur kernels in real-world blurry images, an incremental learning strategy is proposed in [31]. The authors synthesize a large number of blurry-sharp training pairs consisting of different blur kernel sizes. Directly training on a large amount of data can easily lead to the model falling into a local optimal solution. The incremental learning strategy gradually increases the training data and the motion blur kernel size during the training process. The network is first trained on small blur kernels and then progressively expands the training set to add large blur kernels. Then, the network is trained on the set of original and new blur kernels together. Larger blur kernels are continuously added until the training data includes all blur kernels.

6 Evaluation Metrics

Evaluating the output image quality can help us judge the quality of a model. However, it is difficult to construct a sufficiently objective metric that conforms to human perception. In the field of face deblurring, the metrics often used for comparison can be divided into three categories according to different levels and purposes. The first kind of metric aims to give an evaluation from the pixel level of the images; The second kind of metric evaluates the quality of the images from the perspective of visual perception by

extracting the deep features of the images; The third kind of metric is task oriented, which evaluates the quality of images by comparing their accuracy in advanced visual tasks.

6.1 Image level Evaluation Metrics

Among such metrics, the most commonly used are peak signal-to-noise ratio (PSNR) and structural similarity (SSIM). These metrics do not require any additional inputs and can be obtained through some simple calculations. When calculating, they need the ground-truth corresponding to the images, which are reference evaluation metrics.

PSNR: It is acquired by calculating the pixel-level mean squared error of the two images. The larger the value is, the smaller the difference between the two images is. However, the numerical results of PSNR are often inconsistent with the subjective perception of the human vision. Using the PSNR metric tends to lead to over-smoothed results.

SSIM [59]: SSIM is modeled after the visual system of humans. This metric measures the difference between two images in terms of brightness, contrast, and structure. The mean, variance, and covariance of the images are used to evaluate their brightness, contrast, and structural similarity, respectively. The larger the value of SSIM is, the more similar the two images are. However, this metric is also not a good representation of how humans really feel. Images with lower SSIM values may also have a good visual experience.

6.2 Perceptual Evaluation Metrics

These metrics mine deep features in images and can often reflect results consistent with human vision. This includes reference evaluation metrics that require ground-truth and no-reference evaluation metrics that do not require clear images.

LPIPS [60]: Different from the above metrics, LPIPS calculates the distance between two images in the high-dimensional feature space to make the calculation result as close as possible to human visual perception. The high-dimensional deep features are extracted by a pre-trained classification network. LPIPS is a perceptual metric, and a smaller value indicates that two images are visually similar. Its calculation formula is as follows:

$$d(x, x_0) = \sum_l \frac{1}{H_l W_l} \sum_{h,w} \|w_l \odot (\hat{y}_{hw}^l - \hat{y}_{0hw}^l)\|_2^2 \quad (11)$$

Where d is the distance between x and x_0 , \hat{y}_{hw}^l represents the feature extracted from the network, w_l is used to scale channel l and finally the L_2 distance is calculated. Finally, take the average in space and sum on the channel.

NIQE [61]: This metric constructs a set of quality perception features and fits them to a multivariate Gaussian model. The characteristics of quality perception are extracted by Natural Scene Statistics (NSS) model. Then, the quality of the test image is given as the distance between the Multivariate Gauss (MVG) fitting of NSS features extracted from the test image and the MVG model of quality perception features extracted from the natural image corpus. The calculation formula is as follows:

$$D(\nu_1, \nu_2, \Sigma_1, \Sigma_2) = \sqrt{\left((\nu_1 - \nu_2)^T \left(\frac{\Sigma_1 + \Sigma_2}{2} \right)^{-1} (\nu_1 - \nu_2) \right)} \quad (12)$$

Where ν_1, ν_2 and Σ_1, Σ_2 are the mean vector and covariance matrix of natural MVG model and distorted image MVG model. The smaller the value is, the better the image quality is.

In addition, there are many no-reference evaluation metrics for deblurred facial image evaluation, such as: PI [62], BRISQUE [63], NRQM [64], PIQE [65], FID [66], et al.

6.3 Advanced visual task Evaluation Metrics

Image deblurring is a low-level task whose purpose is to improve the accuracy of higher-level tasks, such as: image recognition, object detection, image segmentation, etc. Therefore, for the face deblurring task, a meaningful metric is the identity invariance of deblurred faces and the accuracy of face recognition.

Identity distance. To measure the face identity similarity between deblurred images and ground-truth images, many methods compute their feature distance d_{VGG} in pretrained face recognition networks such as VGG-Face [67]. The smaller the feature distance is, the more similar the face identities in the two images are.

Face detection [31–33, 37]. For detection testing, the OpenFace [68] toolbox is used to measure the success rate of face detection in deblurred images.

Face recognition [27, 31, 33, 37]. For face verification, networks such as MobileNet [69] trained with ArcFace [58] loss are used to compare the face recognition accuracy [70] of the output deblurred images of different methods.

7 Performance Evaluation

Since model-based methods do not require training datasets, it is unfair to directly compare them with learning-based methods. Specifically, model-based methods assist the optimization process by designing a specific prior as a regularization, or building a sample library. However,

learning-based methods often need to train the network on specific datasets to ensure the effect on the test images of same distribution. Therefore, in this section, we compare the experimental performance of representative model-based and deep learning-based methods, respectively.

7.1 Comparison of model-based methods

For traditional methods, we compare sparse prior based methods [71, 72], class-specific prior based methods [12] and exemplar based methods [16]. Also, we compare edge selection based general deblurring methods [73, 74] to these face deblurring methods.

We first show the performance of these methods on synthetic datasets, where test images are selected from the CMU PIE dataset. We choose PSNR and SSIM as evaluation metrics, which are given in the respective papers, and we show them in Table 3. Pan et al. [16] do not release their source code and these two metrics, so we only show their visual performance. To compare the visual effects, we show their qualitative comparison examples in Fig. 12, which are given in [12] as these authors do not provide a full implementation of their methods. The bottom left corner of the recovered image shows the blur kernel estimated by the respective methods.

The methods of Shan et al. [71] and Krishnan et al. [72] produce obvious artifacts as well as multiple edges (ghosting). This is because the sparse prior is a general prior and does not work well on facial images that contain less texture information. The methods of Cho et al. [73] and Xu et al. [74] which are developed for general deblurring estimate denser blur kernel compared to the ground truth. This is because there are not enough sharp edges in the facial image to recover an accurate blur kernel. The exemplar based method of Pan et al. [16] suffers from severe artifacts in the skin texture. This is because they only consider the restoration of the contour of the face without considering the correctness of the internal details of the face. The method of Anwar et al. [12] learns specific priors for different classes by learning the distribution features of different kinds of images in the frequency space. However, the restored images are too smooth and lose the contour information of specific parts.

We also show the performance of representative methods of the above four categories on real blurry images, which are shown in Fig. 13. These images do not have corresponding sharp ground truth. These four classes of methods do not perform well and produce different degrees of artifacts on real images. Furthermore, these methods do not restore sharp results well in areas such as eyes, nose, etc.

Table 3 Performance evaluation of model-based representative methods on CMU PIE dataset. The best results are highlighted in bold.

Method	Type	PSNR(\uparrow)	SSIM(\uparrow)
Shan et al. [71]	Sparse prior	25.59	0.775
Krishnan et al. [72]	Sparse prior	23.54	0.693
Cho et al. [73]	Edge selection	24.38	0.699
Xu et al. [74]	Edge selection	23.30	0.739
Anwar et al. [12]	Class-specific prior	30.75	0.881

**Fig. 12** Qualitative comparisons of representative model-based methods on facial images blurry from CMU PIE dataset. From left to right: blurry image, ground truth, Shan et al. [71], Krishnan et al. [72], Cho et al. [73], Xu et al. [74], Pan et al. [16], Anwar et al. [12].**Table 4** Performance evaluation of representative methods on Shen [31] test dataset. The best results are highlighted in bold.

Method	Type	Helen				CelebA			
		PSNR(\uparrow)	SSIM(\uparrow)	$d_{VGG}(\downarrow)$	LPIPS(\downarrow)	PSNR(\uparrow)	SSIM(\uparrow)	$d_{VGG}(\downarrow)$	LPIPS(\downarrow)
Shen et al. [31]	Supervised	25.58	0.861	91.06	0.1527	24.34	0.860	117.50	0.1832
UMSN [32]	Supervised	27.75	0.897	86.87	0.1086	26.62	0.908	66.33	0.1401
Shen et al. [33]	Supervised	25.91	0.869	-	-	24.89	0.875	-	-
MSPL [34]	Supervised	25.91	0.881	47.80	0.0828	24.91	0.885	57.54	0.0962
Wang et al. [5]	Supervised	22.30	0.775	206.57	0.1592	21.62	0.792	261.50	0.1503
DFPGnet [37]	Supervised	27.70	0.911	42.84	0.0928	26.56	0.915	53.38	0.1052
Lu et al. [45]	Unsupervised	20.25	0.705	241.93	0.1654	19.96	0.742	305.96	0.1688
Xia et al. [47]	Unsupervised	26.13	0.886	55.97	0.1052	25.18	0.892	68.05	0.1199

**Fig. 13** Qualitative comparison of representative model-based methods on real blurry facial images. From left to right: blurry image, Krishnan et al. [72], Xu et al. [74], Pan et al. [16], Anwar et al. [12].

7.2 Comparison of learning-based methods

We compare methods based on semantic segmentation maps, methods based on generative priors, blind face restoration methods, and unsupervised face deblurring methods. We compare the performance of these models on the two most commonly used datasets: Shen et al. dataset [31] and MSPL dataset. The Shen et al. dataset is constructed from the Helen and CelebA datasets, so we compare the performance of above methods on them separately. For evaluation metrics, PSNR and SSIM are the most commonly used metrics, however, they can not represent the most realistic

visual effects. Here, we also choose perceptual metrics LPIPS and VGG distance. These representative methods and their quantitative comparisons are presented in Table 4. Note that all these results are from respective papers.

Shen et al. [33] do not provide their model implementation and their results on perceptual metrics in the paper, so we do not show them here. For pixel-level evaluation metrics such as PSNR and SSIM, the UMSN and DFPGnet models achieve the best and second-best results, respectively. This shows that when used properly, both semantic segmentation maps and generative priors can assist the model to achieve good performance; For perceptual metrics such as d_{VGG} and LPIPS, the DFPGnet and MSPL models achieve the best and second-best results, respectively. This shows that the network based on generative prior can well learn the perceptual similarity between images. In addition, the unsupervised method proposed by Xia et al. achieves performance next only to the above methods and outperforms most unsupervised methods. This model requires two images of the same scene with different degrees of blur as input to make up for the lack of ground truth. This setting can help the training process

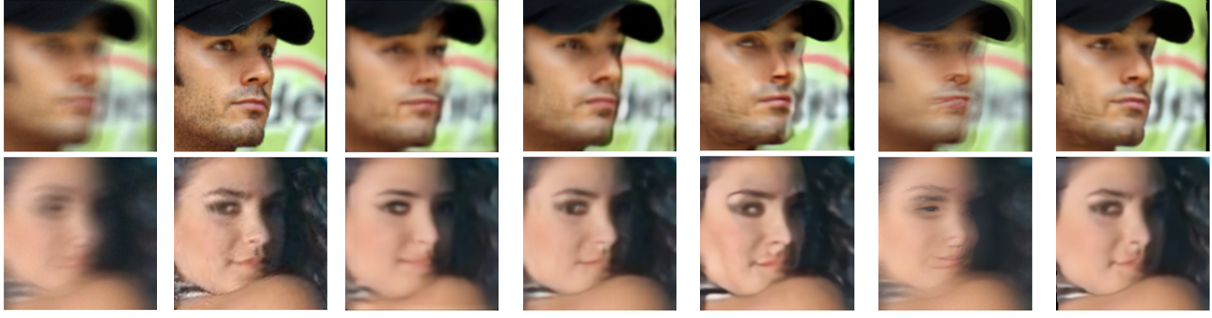


Fig. 14 Qualitative comparison of representative deep learning methods on Shen test dataset [31]. From left to right: blurry image, ground truth, Shen et al. [31], UMSN [32], MSPL [34], Wang et al. [5], DFPG [37].

of the model and make it more robust. That is, trying to add auxiliary images to the unsupervised model is an idea to try. In contrast, unpaired learning methods [45] and multi-task blind face restoration methods [5] achieve poor results.

We also show the qualitative comparison on Shen et al. dataset and MSPL dataset in Fig. 14 and Fig. 15 which is given by [37]. Shen et al. [33] introduced the semantic information of the face as a prior to the network for the first time, and achieved a breakthrough deblurring result. But it produces overly smooth results with unnatural restoration results in small areas like eyes, nose, etc. Models such as UMSN [32] assign different weights to face components, making clear results even on small face components. This shows that introducing the semantic segmentation map into the model and processing different semantic regions separately can improve the performance of the model. However, the model can not recover the blur of the image background well, and the generated faces are somewhat distorted in identity. The representative method DFPGnet, which takes the deep features of the face as a prior, produces deblurring results consistent with the identity of the original image. This shows that the deep features of the image simultaneously contain information such as identity, shape and texture, which can guide the network to generate more realistic results. However, in the facial beard, eyelashes, hair and other parts, models still failed to restore sharp results. As can be seen from Fig. 14, the blind face restoration method [5] produces severe artifacts on the test images. This is because the synthetic training datasets they use only consider the simpler Gaussian blur. So their method can only handle simple and small blurs. The method exhibits poor results when the degradation in the image is severe. As can be seen from Fig. 15, even the best unsupervised methods can not produce comparable results to supervised methods. Restoring sharp images without aligned ground truth remains a difficult problem.

8 Discussion

In this section, we will discuss the main differences between model-based and learning-based methods.

The flexibility of the model. Model-based methods usually need to manually design specific priors which are very important for the final deblurring performance to limit the solution space of the problem. In other words, we often need to design a more refined prior for specific requirements, which is very inflexible. In contrast, deep neural networks can fit complex and varied blur processes due to their powerful fitting capability. Therefore, most of approaches turn to designing more powerful network structures. However, it often requires retraining the network when there are differences in image distribution.

The deblurring performance. Traditional methods usually introduce strong assumptions, such as the existence of a large amount of edge information in the scene. These assumptions result in poor generalization of the model, and ringing and artifacts on severely degraded real blurry images. Benefiting from large model capacity and large-scale datasets, deep learning methods can learn a wide range of blurry patterns, and then produce better results than traditional methods on the test images.

The inference speed. Traditional methods are based on an iterative optimization process, so it takes several minutes to tens of minutes to process one image. In contrast, deep learning methods only need a few milliseconds to process an image at test time.

In summary, learning-based methods outperform traditional methods in terms of flexibility, performance, and inference speed. Therefore, the current mainstream methods are all based on deep learning, and are committed to exploring better network architectures or better training tricks.



Fig. 15 Qualitative comparison of representative deep learning methods on MSPL test dataset [34]. From left to right: blurry image, ground truth, Shen et al. [31], Lu et al. [45], Xia et al. [47], UMSN [32], MSPL [34], DFGP [37].

9 Limitations and Future Research

Deblurring of facial images is a challenging research topic. Here we summarize the problem and limitations of existing methods and provide possible future research directions.

9.1 Model Structure Design

There are four main limitations of the current methods. First, most of the methods can only process spatially uniform blur. In the real world, many scenes have non-uniform blur, such as blur caused by human motion while the background is clear, blurry background but clear foreground caused by using a large aperture of the camera, etc. Most of the existing methods are unable to deal with such spatially non-uniform blur, so identifying the specific blurring degrees of different parts of an image is a problem that needs to be solved; Secondly, the current methods are effective in frontal facial images. However, for side faces, facial images with partial occlusion (such as glasses, hands covering the face), and monitoring equipment images with multiple faces in one image, the result will be severely distorted and anamorphic; Third, when the motion blur is severe, current methods often fail. For severe blurry facial image, these methods will lead to phenomena such as displacement of facial components. Fourth, the recognition accuracy of deblurred facial images is still inferior to that of ground-truth images. The ultimate purpose of deblurring is to improve the accuracy of high-level vision tasks. At present, the most advanced methods have achieved the same accuracy in face detection as clear images. However, in terms of face recognition accuracy (calculated using MobileNet trained with ArcFace loss), there is still a gap of four percentage points between SOTA deblurred images and clear images [37].

For problem 1 and 2, we can seek for the design of finer and better network structure. Many deblurring methods developed for general scenarios have designed models specifically for spatially non-uniform blur [75–77], which can be used as

reference. In order to improve the performance on a variety of facial poses (front or side), it is necessary to explore how to integrate various facial prior, such as semantic segmentation map, generative prior, and 3D prior, into the design of network structure to maximize its effect. For problem 3 and 4, try to increase the model capacity to improve the fitting ability. Nowadays, many transformer-based structures [78, 79] have been developed for image restoration task. With the powerful fitting ability of transformer, the performance of severe blurry images can be improved.

9.2 Construction of datasets

Creating aligned blurry-sharp face image pairs is very difficult. According to this survey, most of the existing datasets are generated by convolving the sharp images with pre-defined blur kernels. There are three main problems. First, synthetic datasets can not represent the distribution of real images in the wild. Second, most of the synthesized blur kernels are spatially invariant, which can not represent dynamic scenes with different blur in different places. Third, many authors build their own dataset, which can be seen in Section 4. They compare their own methods with other methods on their own synthetic dataset, which is unfair. Some methods perform better than others just on specific datasets, but it does not hold while changing to another dataset. Therefore, developing benchmark datasets which cover different blur types is necessary.

9.3 Unsupervised learning

Supervised deep learning methods require a large amount of paired training data to provide supervised information for the model, resulting in data dependence. On the other hand, unpaired learning can be trained on real blurry data without ground-truth, thereby improving the reconstruction ability of the model on real blurry facial images. Therefore, it is necessary to develop unsupervised methods for face deblurring.

Existing unsupervised methods are mainly based on GAN. Since there are no ground-truth images for training, designing proper loss functions is necessary to overcome this disadvantage. These methods also do not fully utilize the semantic or structural information of faces as guidance. When there is no corresponding ground truth image, the extracted semantic information tends to be inaccurate. Therefore, extracting correct semantic information on blurry images and incorporating it into the training of the network is a potential direction for unsupervised learning.

9.4 Model generalizability

The performance improvement of deep learning methods mainly relies on large-capacity models and large datasets. Large-capacity models are extremely computationally expensive during training, and their training results are overly dependent on the training dataset. There are gaps among the distribution of data for people of different skin color, age or ethnicity. Due to this gap between domains, deep learning models have poor generalization performance across different datasets, and are prone to artifacts and other phenomena. Therefore, methods for domain adaptation should be developed and migrated to solve this problem.

9.5 Computational cost

When deeper networks are used to improve performance, model parameters and computational complexity are also improved. It is difficult to deploy these large capacity models on mobile phones or embedded devices of monitoring systems. Therefore, developing lighter face deblurring model while combining and utilizing the characteristics of the device such as dual cameras [80] is a potential future direction.

Declaration of competing interest

The authors have no competing interests to declare that are relevant to the content of this article.

References

- [1] Lu Y. Out-of-focus blur: Image de-blurring. *arXiv preprint arXiv:1710.00620*, 2017.
- [2] Chakrabarti A. A neural approach to blind motion deblurring. In *Computer Vision—ECCV 2016: 14th European Conference, Amsterdam, The Netherlands, October 11–14, 2016, Proceedings, Part III 14*, 2016, 221–235.
- [3] Boracchi G, Foi A. Modeling the Performance of Image Restoration From Motion Blur. *IEEE Transactions on Image Processing*, 2012, 21(8): 3502–3517.
- [4] Song Y, Zhang J, Gong L, He S, Bao L, Pan J, Yang Q, Yang MH. Joint face hallucination and deblurring via structure generation and detail enhancement. *International journal of computer vision*, 2019, 127(6): 785–800.
- [5] Wang X, Li Y, Zhang H, Shan Y. Towards real-world blind face restoration with generative facial prior. In *Proceedings of the IEEE/CVF Conference on Computer Vision and Pattern Recognition*, 2021, 9168–9178.
- [6] Li C. A Survey on Image Deblurring. *arXiv preprint arXiv:2202.07456*, 2022.
- [7] Zhang K, Ren W, Luo W, Lai WS, Stenger B, Yang MH, Li H. Deep image deblurring: A survey. *International Journal of Computer Vision*, 2022: 1–28.
- [8] Nishiyama M, Hadid A, Takeshima H, Shotton J, Kozakaya T, Yamaguchi O. Facial deblur inference using subspace analysis for recognition of blurred faces. *IEEE transactions on pattern analysis and machine intelligence*, 2010, 33(4): 838–845.
- [9] Zhang H, Yang J, Zhang Y, Nasrabadi NM, Huang TS. Close the loop: Joint blind image restoration and recognition with sparse representation prior. In *2011 International Conference on Computer Vision*, 2011, 770–777.
- [10] Tian L, Fan C, Ming Y, Hong X. Weighted non-locally self-similarity sparse representation for face deblurring. In *Asian Conference on Computer Vision*, 2016, 576–589.
- [11] Jiang J, Zhang L, Yang J. Mixed noise removal by weighted encoding with sparse nonlocal regularization. *IEEE transactions on image processing*, 2014, 23(6): 2651–2662.
- [12] Anwar S, Huynh CP, Porikli F. Image deblurring with a class-specific prior. *IEEE transactions on pattern analysis and machine intelligence*, 2018, 41(9): 2112–2130.
- [13] Zhang M, Fang Y, Ni G, Zeng T. Pixel Screening Based Intermediate Correction for Blind Deblurring. In *Proceedings of the IEEE/CVF Conference on Computer Vision and Pattern Recognition*, 2022, 5892–5900.
- [14] Tian D, Tao D. Coupled learning for facial deblur. *IEEE Transactions on Image Processing*, 2015, 25(2): 961–972.
- [15] Mittal A, Moorthy AK, Bovik AC. Making image quality assessment robust. In *2012 Conference Record of the Forty Sixth Asilomar Conference on Signals, Systems and Computers (ASILOMAR)*, 2012, 1718–1722.
- [16] Pan J, Hu Z, Su Z, Yang MH. Deblurring face images with exemplars. In *European conference on computer vision*, 2014, 47–62.
- [17] Hachohen Y, Shechtman E, Lischinski D. Deblurring by Example Using Dense Correspondence. In *2013 IEEE International Conference on Computer Vision*, 2013, 2384–2391.
- [18] Szegedy C, Liu W, Jia Y, Sermanet P, Reed S, Anguelov D, Erhan D, Vanhoucke V, Rabinovich A. Going deeper with convolutions. In *Proceedings of the IEEE conference on computer vision and pattern recognition*, 2015, 1–9.
- [19] Ronneberger O, Fischer P, Brox T. U-net: Convolutional networks for biomedical image segmentation. In *Internation*

- tional Conference on Medical image computing and computer-assisted intervention, 2015, 234–241.
- [20] Nah S, Hyun Kim T, Mu Lee K. Deep multi-scale convolutional neural network for dynamic scene deblurring. In *Proceedings of the IEEE conference on computer vision and pattern recognition*, 2017, 3883–3891.
- [21] Goodfellow I, Pouget-Abadie J, Mirza M, Xu B, Warde-Farley D, Ozair S, Courville A, Bengio Y. Generative adversarial nets. *Advances in neural information processing systems*, 2014, 27.
- [22] Schuler CJ, Hirsch M, Harmeling S, Schölkopf B. Learning to deblur. *IEEE transactions on pattern analysis and machine intelligence*, 2015, 38(7): 1439–1451.
- [23] Jin M, Hirsch M, Favaro P. Learning Face Deblurring Fast and Wide. In *2018 IEEE/CVF Conference on Computer Vision and Pattern Recognition Workshops (CVPRW)*, 2018, 858–8588.
- [24] He K, Zhang X, Ren S, Sun J. Deep residual learning for image recognition. In *Proceedings of the IEEE conference on computer vision and pattern recognition*, 2016, 770–778.
- [25] Lin S, Zhang J, Pan J, Liu Y, Wang Y, Chen J, Ren J. Learning to Deblur Face Images via Sketch Synthesis. *Proceedings of the AAAI Conference on Artificial Intelligence*, 2020, 34(07): 11523–11530.
- [26] Xu L, Ren JS, Liu C, Jia J. Deep convolutional neural network for image deconvolution. *Advances in neural information processing systems*, 2014, 27.
- [27] Chrysos GG, Favaro P, Zafeiriou S. Motion Deblurring of Faces. *International Journal of Computer Vision*, 2019, 127(6-7): 801–823.
- [28] Chrysos GG, Zafeiriou S. Deep Face Deblurring. In *2017 IEEE Conference on Computer Vision and Pattern Recognition Workshops (CVPRW)*, 2017, 2015–2024.
- [29] Wang L, Li Y, Wang S. DeepDeblur: fast one-step blurry face images restoration. *arXiv preprint arXiv:1711.09515*, 2017.
- [30] Qi Q, Guo J, Li C, Xiao L. Blind Face Images Deblurring with Enhancement. *Multimedia Tools and Applications*, 2021, 80(2): 2975–2995.
- [31] Shen Z, Lai WS, Xu T, Kautz J, Yang MH. Deep Semantic Face Deblurring. In *2018 IEEE/CVF Conference on Computer Vision and Pattern Recognition*, 2018, 8260–8269.
- [32] Yasarla R, Perazzi F, Patel VM. Deblurring face images using uncertainty guided multi-stream semantic networks. *IEEE Transactions on Image Processing*, 2020, 29: 6251–6263.
- [33] Shen Z, Lai WS, Xu T, Kautz J, Yang MH. Exploiting Semantics for Face Image Deblurring. *International Journal of Computer Vision*, 2020, 128(7): 1829–1846.
- [34] Lee TB, Jung SH, Heo YS. Progressive Semantic Face Deblurring. *IEEE Access*, 2020, 8: 223548–223561.
- [35] Ren W, Yang J, Deng S, Wipf D, Cao X, Tong X. Face Video Deblurring Using 3D Facial Priors. In *2019 IEEE/CVF International Conference on Computer Vision (ICCV)*, 2019, 9387–9396.
- [36] Zhu F, Zhu J, Chu W, Zhang X, Ji X, Wang C, Tai Y. Blind Face Restoration via Integrating Face Shape and Generative Priors. In *Proceedings of the IEEE/CVF Conference on Computer Vision and Pattern Recognition*, 2022, 7662–7671.
- [37] Jung SH, Bok Lee T, Heo YS. Deep Feature Prior Guided Face Deblurring. In *2022 IEEE/CVF Winter Conference on Applications of Computer Vision (WACV)*, 2022, 884–893.
- [38] Zhang X, Zhang H, Lv J, Li X. Face Deblurring Based on Separable Normalization and Adaptive Denormalization. *arXiv preprint arXiv:2112.09833*, 2021.
- [39] Lin TY, Goyal P, Girshick R, He K, Dollár P. Focal loss for dense object detection. In *Proceedings of the IEEE international conference on computer vision*, 2017, 2980–2988.
- [40] Hu X, Ren W, Yang J, Cao X, Wipf DP, Menze B, Tong X, Zha H. Face Restoration via Plug-and-Play 3D Facial Priors. *IEEE Transactions on Pattern Analysis and Machine Intelligence*, 2021.
- [41] Paysan P, Knothe R, Amberg B, Romdhani S, Vetter T. A 3D face model for pose and illumination invariant face recognition. In *2009 sixth IEEE international conference on advanced video and signal based surveillance*, 2009, 296–301.
- [42] Xu X, Sun D, Pan J, Zhang Y, Pfister H, Yang MH. Learning to super-resolve blurry face and text images. In *Proceedings of the IEEE international conference on computer vision*, 2017, 251–260.
- [43] Karras T, Laine S, Aittala M, Hellsten J, Lehtinen J, Aila T. Analyzing and improving the image quality of stylegan. In *Proceedings of the IEEE/CVF conference on computer vision and pattern recognition*, 2020, 8110–8119.
- [44] Madam NT, Kumar S, Rajagopalan AN. Unsupervised Class-Specific Deblurring. In V Ferrari, M Hebert, C Sminchisescu, Y Weiss, editors, *Computer Vision – ECCV 2018*, volume 11214, 2018, 358–374.
- [45] Lu B, Chen JC, Chellappa R. Unsupervised Domain-Specific Deblurring via Disentangled Representations. In *2019 IEEE/CVF Conference on Computer Vision and Pattern Recognition (CVPR)*, 2019, 10217–10226.
- [46] Zhu JY, Park T, Isola P, Efros AA. Unpaired image-to-image translation using cycle-consistent adversarial networks. In *Proceedings of the IEEE international conference on computer vision*, 2017, 2223–2232.
- [47] Xia Z, Chakrabarti A. Training image estimators without image ground truth. *Advances in Neural Information Processing Systems*, 2019, 32.
- [48] Huber PJ. Robust regression: asymptotics, conjectures and Monte Carlo. *The annals of statistics*, 1973: 799–821.
- [49] Lai WS, Huang JB, Hu Z, Ahuja N, Yang MH. A Comparative Study for Single Image Blind Deblurring. In *2016 IEEE Conference on Computer Vision and Pattern Recognition (CVPR)*, 2016, 1701–1709.
- [50] Le V, Brandt J, Lin Z, Bourdev L, Huang TS. Interactive Facial Feature Localization. In D Hutchison, T Kanade, J Kittler, JM Kleinberg, F Mattern, JC Mitchell, M Naor, O Nierstrasz, C Pandu Rangan, B Steffen, M Sudan, D Terzopoulos, D Tygar, MY Vardi, G Weikum, A Fitzgibbon, S Lazebnik, P Perona,

- Y Sato, C Schmid, editors, *Computer Vision – ECCV 2012*, volume 7574, 2012, 679–692.
- [51] Terence Sim, Baker S, Bsat M. The CMU Pose, Illumination, and Expression Database. *IEEE Transactions on Pattern Analysis and Machine Intelligence*, 2003, 25(12): 1615–1618.
- [52] Liu Z, Luo P, Wang X, Tang X. Deep learning face attributes in the wild. In *Proceedings of the IEEE international conference on computer vision*, 2015, 3730–3738.
- [53] Lee CH, Liu Z, Wu L, Luo P. MaskGAN: Towards Diverse and Interactive Facial Image Manipulation. In *2020 IEEE/CVF Conference on Computer Vision and Pattern Recognition (CVPR)*, 2020, 5548–5557.
- [54] Karras T, Laine S, Aila T. A style-based generator architecture for generative adversarial networks. In *Proceedings of the IEEE/CVF conference on computer vision and pattern recognition*, 2019, 4401–4410.
- [55] Ng HW, Winkler S. A data-driven approach to cleaning large face datasets. In *2014 IEEE international conference on image processing (ICIP)*, 2014, 343–347.
- [56] Kumar N, Berg AC, Belhumeur PN, Nayar SK. Attribute and Simile Classifiers for Face Verification. In *2009 IEEE 12th International Conference on Computer Vision*, 2009, 365–372.
- [57] Gross R, Matthews I, Cohn J, Kanade T, Baker S. Multi-pie. *Image and vision computing*, 2010, 28(5): 807–813.
- [58] Deng J, Guo J, Xue N, Zafeiriou S. Arcface: Additive angular margin loss for deep face recognition. In *Proceedings of the IEEE/CVF conference on computer vision and pattern recognition*, 2019, 4690–4699.
- [59] Wang Z, Bovik A, Sheikh H, Simoncelli E. Image Quality Assessment: From Error Visibility to Structural Similarity. *IEEE Transactions on Image Processing*, 2004, 13(4): 600–612.
- [60] Zhang R, Isola P, Efros AA, Shechtman E, Wang O. The Unreasonable Effectiveness of Deep Features as a Perceptual Metric. In *2018 IEEE/CVF Conference on Computer Vision and Pattern Recognition*, 2018, 586–595.
- [61] Mittal A, Soundararajan R, Bovik AC. Making a “Completely Blind” Image Quality Analyzer. *IEEE Signal Processing Letters*, 2013, 20(3): 209–212.
- [62] Ignatov A, Timofte R, Van Vu T, Luu TM, Pham TX, Van Nguyen C, Kim Y, Choi JS, Kim M, Huang J, Ran J, Xing C, Zhou X, Zhu P, Geng M, Li Y, Agustsson E, Gu S, Van Gool L, de Stoutz E, Kobyshev N, Nie K, Zhao Y, Li G, Tong T, Gao Q, Hanwen L, Micheline PN, Dan Z, Fengshuo H, Hui Z, Wang X, Deng L, Meng R, Qin J, Shi Y, Wen W, Lin L, Feng R, Wu S, Dong C, Qiao Y, Vasu S, Thekke Madam N, Kandula P, Rajagopalan AN, Liu J, Jung C. PIRM Challenge on Perceptual Image Enhancement on Smartphones: Report. In L Leal-Taixé, S Roth, editors, *Computer Vision – ECCV 2018 Workshops*, volume 11133, 2019, 315–333.
- [63] Mittal A, Moorthy AK, Bovik AC. No-Reference Image Quality Assessment in the Spatial Domain. *IEEE Transactions on Image Processing*, 2012, 21(12): 4695–4708.
- [64] Ma C, Yang CY, Yang X, Yang MH. Learning a no-reference quality metric for single-image super-resolution. *Computer Vision and Image Understanding*, 2017, 158: 1–16.
- [65] N V, D P, Bh MC, Channappayya SS, Medasani SS. Blind Image Quality Evaluation Using Perception Based Features. In *2015 Twenty First National Conference on Communications (NCC)*, 2015, 1–6.
- [66] Heusel M, Ramsauer H, Unterthiner T, Nessler B, Hochreiter S. GANs Trained by a Two Time-Scale Update Rule Converge to a Local Nash Equilibrium. In *Advances in Neural Information Processing Systems*, volume 30, 2017.
- [67] Parkhi OM, Vedaldi A, Zisserman A. Deep face recognition, 2015.
- [68] Amos B, Ludwiczuk B, Satyanarayanan M, et al.. Openface: A general-purpose face recognition library with mobile applications. *CMU School of Computer Science*, 2016, 6(2): 20.
- [69] Howard AG, Zhu M, Chen B, Kalenichenko D, Wang W, Weyand T, Andreetto M, Adam H. Mobilenets: Efficient convolutional neural networks for mobile vision applications. *arXiv preprint arXiv:1704.04861*, 2017.
- [70] Huang GB, Mattar M, Berg T, Learned-Miller E. Labeled faces in the wild: A database for studying face recognition in unconstrained environments. In *Workshop on faces in 'Real-Life' Images: detection, alignment, and recognition*, 2008.
- [71] Shan Q, Jia J, Agarwala A. High-quality motion deblurring from a single image. *Acm transactions on graphics (tog)*, 2008, 27(3): 1–10.
- [72] Krishnan D, Tay T, Fergus R. Blind deconvolution using a normalized sparsity measure. In *CVPR 2011*, 2011, 233–240.
- [73] Cho S, Lee S. Fast motion deblurring. In *ACM SIGGRAPH Asia 2009 papers*, 2009, 1–8.
- [74] Xu L, Jia J. Two-phase kernel estimation for robust motion deblurring. In *European conference on computer vision*, 2010, 157–170.
- [75] Zhang J, Pan J, Ren J, Song Y, Bao L, Lau RW, Yang MH. Dynamic scene deblurring using spatially variant recurrent neural networks. In *Proceedings of the IEEE Conference on Computer Vision and Pattern Recognition*, 2018, 2521–2529.
- [76] Gao H, Tao X, Shen X, Jia J. Dynamic scene deblurring with parameter selective sharing and nested skip connections. In *Proceedings of the IEEE/CVF conference on computer vision and pattern recognition*, 2019, 3848–3856.
- [77] Yuan Y, Su W, Ma D. Efficient dynamic scene deblurring using spatially variant deconvolution network with optical flow guided training. In *Proceedings of the IEEE/CVF Conference on Computer Vision and Pattern Recognition*, 2020, 3555–3564.
- [78] Zamir SW, Arora A, Khan S, Hayat M, Khan FS, Yang MH. Restormer: Efficient transformer for high-resolution image restoration. In *Proceedings of the IEEE/CVF Conference on Computer Vision and Pattern Recognition*, 2022, 5728–5739.
- [79] Chen H, Wang Y, Guo T, Xu C, Deng Y, Liu Z, Ma S, Xu C,

- Xu C, Gao W. Pre-trained image processing transformer. In *Proceedings of the IEEE/CVF Conference on Computer Vision and Pattern Recognition*, 2021, 12299–12310.
- [80] Lai WS, Shih Y, Chu LC, Wu X, Tsai SF, Krainin M, Sun D, Liang CK. Face deblurring using dual camera fusion on mobile phones. *ACM Transactions on Graphics (TOG)*, 2022, 41(4): 1–16.